Conductance regimes in superconducting junctions of atomic size

J.G. Rodrigo, N. Agraït, and S. Vieira
Laboratorio de Bajas Temperaturas, Departamento Física de la Materia Condensada, C-III, Universidad Autónoma de Madrid, 28049 Madrid, Spain
(Received 14 January 1994)

A scanning tunneling microscope has been used to study the different conductance regimes of superconducting Pb junctions of atomic size. Measurement of the apparent tunneling barrier and imaging of probed areas before and after the spectroscopic measurement give information on the surface condition and the geometry of the junction. The evolution of the differential conductance curves is followed from the tunneling regime to contact as the junction is varied in a continuous and controlled manner. The observed evolution of the conductance follows quantitatively Octavio-Tinkham-Blonder-Klapwijk theory with the addition of a lifetime broadening parameter, which accounts for the observed smearing of the superconducting gap features.

I. INTRODUCTION

Considerable information about electronic and lattice properties of conducting materials has been obtained during the last years using electron tunneling techniques. Planar junctions, point contact, and various other geometries have been used to determine the electronic density of states of various superconductors, as well as the phonon spectrum.[1]

The scanning tunneling microscope (STM) opens new possibilities. STM can be used not only as a sophisticated point-contact device allowing for a controlled variation of the junction resistance from several megaohm in the tunneling regime down to a few ohms in the contact regime,[2,3] but also as a probe of the superconducting properties that can be correlated to topographic features in an atomic scale.[4,5] However, tunneling spectroscopy gives information not only of the electronic properties of the electrode materials but also of the barrier between them. Knowledge of the effect of the barrier in the current vs voltage curves (IV characteristics) is essential for the interpretation of the results obtained with small-size variable junctions like those produced by STM.

Blonder, Tinkham, and Klapwijk[6] studied theoretically the conductance of normal-metal–superconductor (NS) junctions including an arbitrary probability of scattering at the NS interface to account for the variation of the barrier strength. They showed that some of the features observed in the point-contact experimental IV characteristics,[7] like the enhanced conductance at zero bias and the excess current, can be explained by the Andreev reflection mechanism. Octavio, Tinkham, Blonder, and Klapwijk[8] (OTBK) showed that this mechanism also explains the subharmonic gap structure of superconductor-superconductor (SS) junctions. Experimental point-contact results[9] are only in qualitative agreement with this theory possibly due to the lack of homogeneity of the barrier.

We think that a specific study of the effect of the barrier in actual atomic size STM junctions in a well-known superconductor, taking account of the OTBK theory and exploiting the capabilities of STM, will allow a deep understanding of the involved phenomena. This study would be useful for the analysis of experiments with other superconducting materials using similar tools, and, in particular, for the interpretation of the results obtained in copper oxide superconductors,[10,11] for which many discrepancies are found in the literature.

In this paper we present a detailed study of the different conductance regimes, using STM, as the barrier of the junction is varied, for a well-known superconductor: lead, which is a strong coupling type-I superconductor with a superconducting gap at the Fermi level, $\Delta_0 = 1.35$ meV, and a critical temperature $T_c = 7.19$ K. Many studies have been done on this material and its microscopic superconducting properties are well understood within the BCS framework. Both our tip and substrate are made out of lead, and consequently we have a SS junction. We have chosen this junction instead of the simpler NS junction, because the conductance shows a much richer structure (variable height of the Andreev hump, and subharmonic gap structure), that will help us in the identification of the different regimes.

II. EXPERIMENTAL RESULTS

The experimental setup used in our experiment is the same as in previous studies.[3,12,13] The tip and substrate are both polycrystalline Pb, and all the measurements presented in this paper were taken at 5.5 K. Substrate surface and tip are both scratched clean right before cooling, and the experiment is performed in helium exchange gas. Series of IV curves are acquired by changing the z-piezo voltage in small increments. During the acquisition of each individual curve the z-piezo voltage is fixed while the bias voltage is ramped in 20 ms, and 1024 current data points are measured. Voltage is typically ramped between ± 40 mV and voltage resolution is 80 μV. The spectrum (differential conductance curves) is

0163-1829/94/50(1)/374(6)/$06.00

computed numerically. Each series typically spans the tunneling and contact regimes reaching areas of up to 5000 Å (about 10Ω). Similarly, I-z curves are acquired at constant bias voltage by ramping the z-piezo voltage.

Figure 1(a) shows a typical 500 × 500 Å^2 area of the substrate. The lateral resolution is not very high, indicating that the tip is somewhat blunt. After taking several IV curves with R_N=200Ω the same area was imaged again and the substrate showed no modification [this image is not shown because it is identical to Fig. 1(a)]. Figure 1(b) shows the same area after taking several IV curves at R_N=20 Ω. In this case a protrusion of about 100 Å diameter appears at the spot where contact was established. The electrical resistance of a clean contact is related to the contact radius by Sharvin equation, $R_0 = 4\rho l/3A = 4(h/2e^2)\pi/Ak_F^2$ where ρ is the resistivity; l is the mean free path; A is the area of the contact; k_F is the Fermi wave number; and h is Planck's constant. Thus, a resistance of 20Ω corresponds to a contact radius of 33 Å, which is consistent with the observed size of the protrusion (the size of the protrusion cannot be measured precisely, since a blunt tip will make it look larger). The formation of this protrusion due to cohesive bonding between tip and substrate and the formation and subsequent break of a connective neck[12] indicates that the contacting surfaces are clean since for contaminated contacts adhesive bonding is much weaker.[14,15]

The current vs distance curves (I-z curves) at constant voltage bias give information on the apparent barrier of the junction. In Fig. 2 we have plotted $\log_{10} I/V$ vs z. The resulting apparent barrier,[16] defined as $\phi_{ap} = 0.952(d \ln I/dz)^2$, attains a high value ($\phi_{ap}$=3.5 eV) in the tunneling regime ($R_N \geq 100$ kΩ). Such high apparent tunneling barriers close to the work function (3.8 eV) of the material are usually taken as indicative of the cleanliness of the surfaces.[14,17] Closer to the substrate the jump-to-contact phenomenon[14,17] causes a sudden increase in the current. For resistances of about 10 kΩ the barrier collapses and subsequent variations in the current are attained by discrete area variations.[12,13]

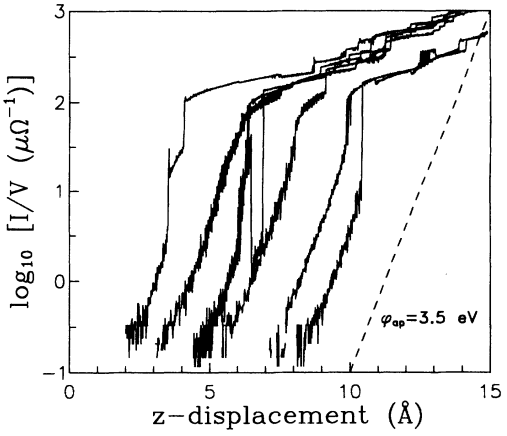

FIG. 2. $\log_{10} I/V$ vs z curves for a clean junction showing the transition from tunneling to contact. (Note that 0 in the vertical axis corresponds to R_N=1 MΩ, 1 to R_N=100 kΩ, etc.)

The experimental evolution of the spectra for SS junctions for resistances ranging from 100 kΩ to 2Ω is shown in Fig. 3. Curves obtained for larger resistances (up to 100 MΩ) are identical to that of 100 kΩ and are not shown. Different series taken at the same spot differ slightly in the resistance for which the first contact is established (see Fig. 4), indicating different atomic arrangements at the tip apex.

We have studied *hundreds* of spots of nine different substrates and tips, and we find that the above described behavior is representative of situations in which the substrate can be imaged without any problem, the apparent barrier is high and the jump-to-contact phenomenon is

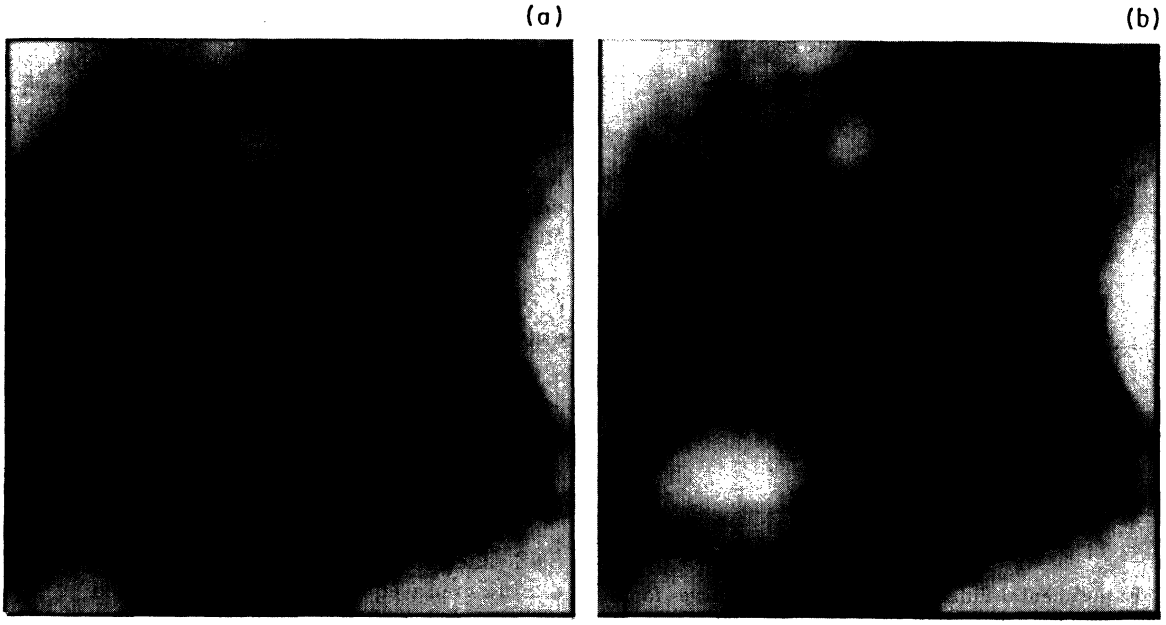

FIG. 1. A typical 50 × 50 nm^2 area of the Pb substrate at 5.5 K. (a) Before taking any IV curve; (b) after taking several IV curves at 20Ω resistance.

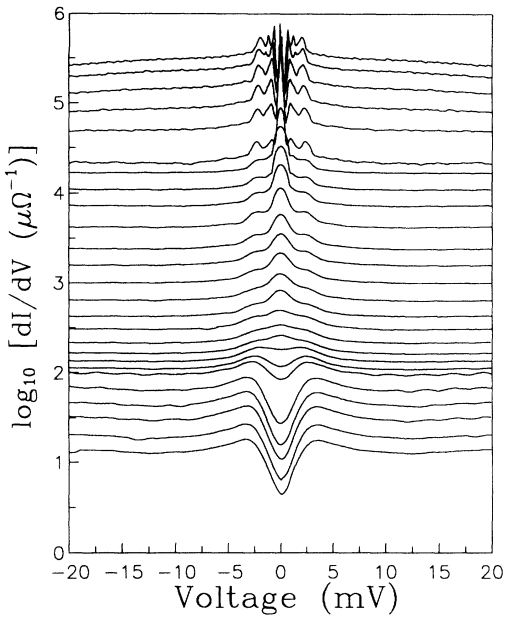

FIG. 3. Experimental differential conductance curves for a clean Pb-Pb junction (complete series). Note log vertical scale.

clearly observed. The difference between the series of spectra taken at different spots is not bigger than that shown in Fig. 4. This behavior is consistent with a clean junction, in which the surfaces of tip and substrate are free from contamination (except, possibly, an adsorbed helium layer that is easily pushed apart as the gap between tip and subatrate decreases).

Figures 2 and 3 allow us to correlate the different conductance regimes with the tip-to-substrate distance and apparent barrier. For separations larger than 3–4 Å, the apparent barrier is large (tunneling regime) and the superconducting gap structure is clearly observed. As tip-to-substrate distance diminishes the resistance jumps

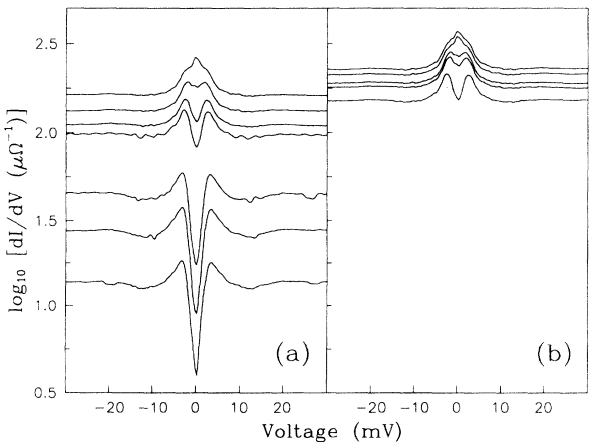

FIG. 4. Experimental differential conductance curves for a clean Pb-Pb junction, for two different junctions. The vertical offset indicates a difference in conductance at the point where the barrier collapses of about 50%.

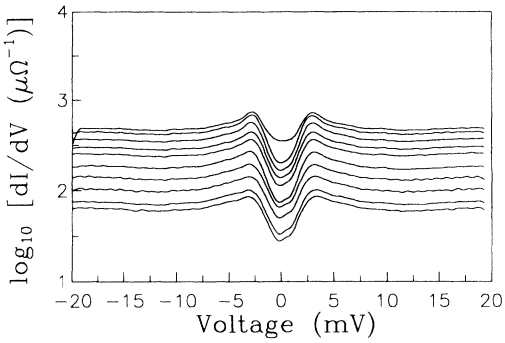

FIG. 5. Experimental differential conductance curves for a dirty Pb-Pb junction. Notice the conductance scale which is *not* arbitrary and the vertical scale is to be directly compared to that of Fig. 3.

from about 100 kΩ in the tunneling regime to about 10 kΩ as mechanical contact is established (jump-to-contact phenomenon). In Fig. 4(a), the jump to contact took place between curves 3 and 4 (counting from below). We can see that mechanical contact has been established but the barrier is not totally collapsed and the superconducting gap is still visible (see next section). Between 10 and 5 kΩ the barrier collapses and the zero-bias hump due to Andreev reflection is fully developed (Figs. 3 and 4). As the tip is further pressed into the substrate the contact area increases by plastic deformation, the subharmonic gap structure becomes clearer and finally a Josephson peak appears. This Josephson regime will be considered in full detail elsewhere.[19]

The presence of contamination between tip and substrate, due for instance to improper cleaning, can be readily detected: imaging is difficult or impossible, the apparent barrier presents much lower values, and irreproducible sudden jumps in the current occur for large tip-to-substrate resistances (> 100 kΩ). Moreover, the series of *IV* curves are rather irreproducible. In Fig. 5 we show one such series corresponding to this situation, a contamination layer prevents direct contact between tip and sample, pressing the tip against the substrate results in a larger area rather than diminishing the tunneling barrier, and no Andreev peak appears. Note that these curves cover the resistance range in which the collapse of the barrier occurred in Fig. 3.

III. DISCUSSION OF THE RESULTS

The experimental spectra in Figs. 3 and 5 can be modeled accurately using OTBK theory,[8] with the addition of a phenomenological lifetime broadening parameter, Γ, to account for the smearing of the features observed in the experimental spectra.[3,18]

In OTBK theory the SS junction is modeled as a SNS junction with scattering at both NS interfaces and a Boltzmann equation approach is used to obtain the conductance. The coefficients for Andreev reflection, normal reflection, and transmission are computed using Bogoliubov–de Gennes equations. The elastic scatter-

ing processes at each NS interface are simulated by a δ function potential $H\delta(x)$, and the strength of the barrier is given in terms of a nondimensional parameter $Z = H/\hbar v_F$, where v_F is Fermi velocity. The normal state resistance is given by $R_N = R_0(1 + 2Z^2)$, where R_0 is given by Sharvin resistance, which is inversely proportional to the area of the junction. This model is one dimensional, and Josephson effects, heating, charge imbalance, and strong coupling effects, are neglected, but it contains the essential physical processes in the transition from moderate to low barrier strengths. For large values of Z the model is not satisfactory.[8]

The lifetime parameter, Γ, is easily introduced by using a complex energy $E \to E + i\Gamma$.[3,18] The computational procedure is the same as that in Ref. 8. Comparing the shape of the theoretical and experimental series of curves we assign a value of Γ and Z to each experimental curve. The fitting procedure is performed with normalized conductance curves, paying attention to match the shape, peaks, and bottom values of the theoretical and experimental series. Strong coupling effects which lead to the features in the conductance curves for energies about 2Δ are not taken into account in the modeling procedure. The resulting accuracy in Γ and Z is 10–20%.

In Fig. 6, we show the experimental and theoretical spectra for three different sets of curves corresponding to the clean series of Fig. 3. The large resistance spectra corresponding to the tunneling regime, Fig. 6(a), present no variation for a wide range of resistance (from 100 MΩ to 100 kΩ). Note the phonon structure around ±10 meV due to strong coupling effects. This curve is modeled using the lifetime broadening model[18] with $\Gamma = 0.4$ meV. In the transition region, Fig. 6(b), Z varies fast because the barrier is collapsing, and Γ also diminishes but more slowly. In the contact region the barrier strength is almost constant $Z = 0.4$ and Γ goes to zero as the area of

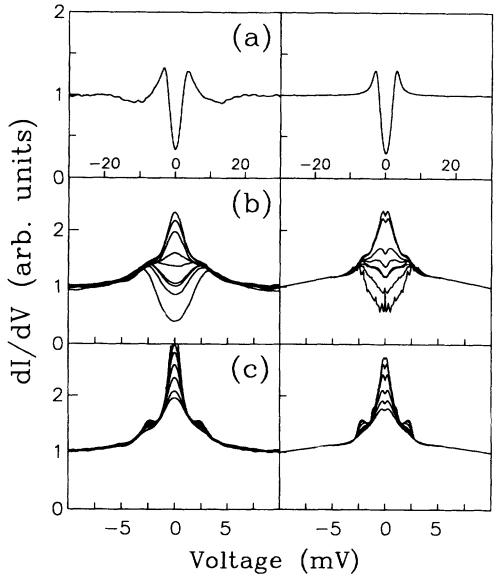

FIG. 6. Normalized experimental conductance curves (left) for the three different regions of conductance and the corresponding theoretical curves (right) modeled using: (a) lifetime broadening model with $\phi_{ap} = 3.5$ eV and Γ=0.4 meV; (b) and (c) modified OTBK model. The pairs [Z,Γ (meV)] corresponding to these curves are (2, 0.4), (1, 0.4), (0.7, 0.4), (0.7, 0.3), (0.6, 0.3), (0.5, 0.3), (0.4, 0.2), (0.4, 0.15) for (b) (0.4, 0.4), (0.4, 0.3), (0.4, 0.2), (0.4, 0.1), (0.4, 0.05), (0.4, 0.025), (0.4, 0) for (c). The features at zero bias are computational artifacts.

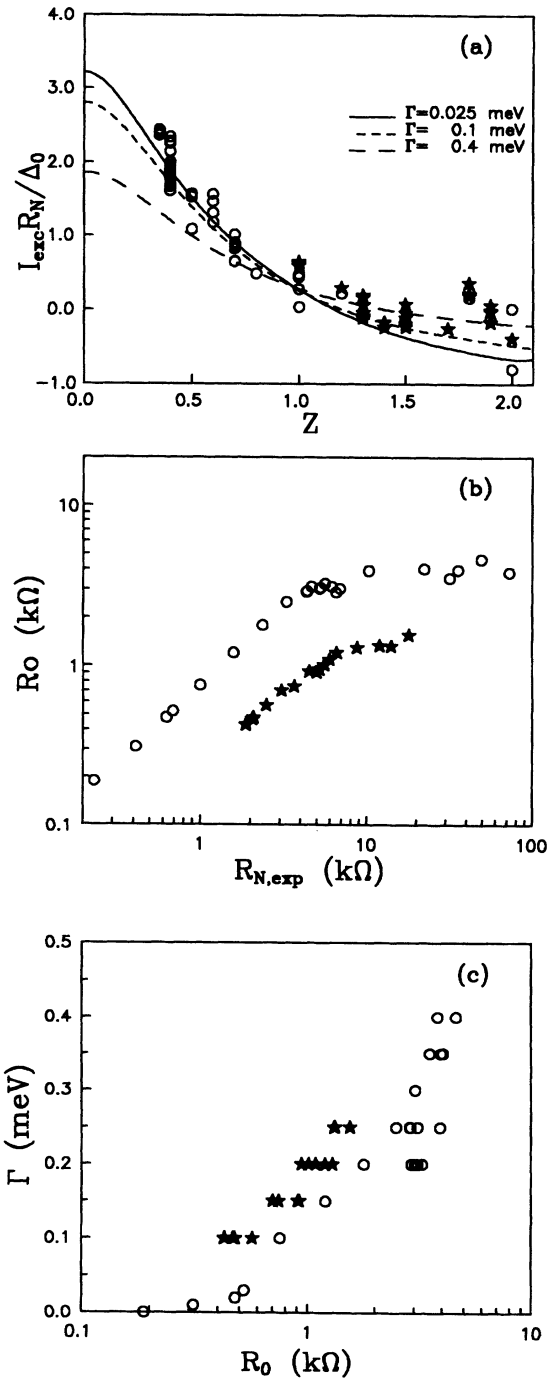

FIG. 7. (a) Experimental excess current vs Z and OTBK theoretical curves for three different values of Γ. (b) R_0 ($\propto 1/A$) variation in the transition from tunneling to contact. (c) Γ vs R_0 behavior for the experimental series. Circles correspond to the curves in Fig. 3, stars correspond to the curves in Fig. 5.

the contact increases, Fig. 6(c). This nonzero value of Z when tip and substrate are in contact may arise from irregularities in the constriction or any mismatch between the electrodes.[7]

We can check the consistency in these assigned values of Z and Γ comparing the experimental normalized excess current with the prediction of OTBK model [see Fig. 7(a)].

The area of the junction corresponding to each curve can be obtained from the experimental normal resistance, $R_{N,\mathrm{expt}}$, and the assigned value of Z, since $R_0 = R_{N,\mathrm{expt}}/1 + 2Z^2$, and R_0 is the Sharvin resistance for a circular contact which is inversely proportional to the area. The circles in Fig. 7(b) show R_0 vs $R_{N,\mathrm{expt}}$ for the series in Fig. 3. Before contact, $R_{N,\mathrm{expt}} > 10\mathrm{k}\ \Omega$, R_0 is constant, and the corresponding area is 16 Å^2 [or about 1 atom (Ref. 20)]. The region 10 k$\Omega > R_{N,\mathrm{expt}} > 5$ kΩ corresponds to the transition region where contact is established and the gap structure turns into the Andreev hump [see Figs. 3, 4(a), and 2]. As the tip is further pressed against the substrate, the contact area increases, Z remains constant, R_0 decreases linearly with $R_{N,\mathrm{expt}}$ (slope 1 in log-log plot).

The variation of the phenomenological parameter Γ, used in the modeling to account for the broadening of the spectra for the series in Fig. 3 is shown in Fig. 7(c). For large values of $R_{N,\mathrm{expt}}$, both R_0 and Γ are almost constant and attain their maximum values (about 4 kΩ and 0.4 meV, respectively). Only after contact is established Γ diminishes as R_0 decreases (junction effective area increases) being practically zero for areas larger than about 15 atoms. Note that most of the variation of Γ occurs when the barrier has already collapsed (Z has reached its minimum value), and consequently Γ depends only on the area of the junction.

The series corresponding to a dirty junction (Fig. 5) is represented as stars in Fig. 7.[21] Figure 7(b) shows that, for the same value of $R_{N,\mathrm{expt}}$, the area of the dirty junctions is about three times larger than for the clean junctions. In Fig. 7(a) we see that these curves also have an excess current consistent with the model, and that the minimum value of Z is 1. This behavior is consistent with the presence of a contamination layer between the electrodes which prevents direct contact, and leads to a rather high minimum value of Z and to an increase of the junction area when we press tip and sample. These curves, however, show the same behavior in Γ vs R_0 [Fig. 7(c)] to those corresponding to the clean case, which supports our previous statement that Γ depends only on area of the junction.

Our results show that pair breaking due to high current density or nonequilibrium effects[5,22] cannot be invoked to account for the smearing in the observed experimental spectra of superconducting junctions of atomic size since for the larger current densities $\Gamma = 0$. The effect of surface contamination[5] can also be discarded because we observe smearing both for clean or dirty junctions in our experiment. Scattering effects in this constriction of atomic size, or at the surfaces could be responsible for the observed smearing.

IV. CONCLUSIONS

The utilization of STM makes possible a continuous evolution of an atomic size junction from tunneling to contact regime covering a variation in the resistance of the junction of more than 6 orders of magnitude.

When the surfaces of tip and substrate are clean the apparent barrier in the tunneling regime is high, and contact is established at about 10 kΩ. In this case the series of spectra are totally reproducible, and the different series differ only in the point for which the barrier collapses (but always from 5 to 10 kΩ) due to different atomic arrangements at the tip apex. Imaging the substrate after a series of IV curves shows surface modifications induced by adhesive contact formation, which indicate a contact diameter consistent with the diameter deduced from the electrical resistance of the junction.

The presence of contamination between tip and substrate results in difficulties for imaging the substrate, low apparent barriers, and irreproducible series of spectra.

Both for clean and contaminated junctions the conductance curves of these nanoscopic superconducting junctions follow quantitatively the behavior described by OTBK theory modified by the introduction of a phenomenological lifetime broadening parameter. From the resulting continuous evolution of the spectra the area of the junction corresponding to each spectrum is obtained without ambiguity. By correlating the current variations with distance and the evolution of the spectra for clean junctions, we see that the tunneling barrier starts to collapse after the point of mechanical contact.

ACKNOWLEDGMENTS

We thank C. Sirvent for his collaboration in the preparation of the experiment. This work has been supported by the Comunidad de Madrid under Contract No. C031/90, and by the CICYT under Contract No. MAT92-0170.

[1] E.L. Wolf, *Principles of Electron Tunneling Spectroscopy* (Oxford University Press, New York, 1985); K.K. Likharev, Rev. Mod. Phys. **51,** 101 (1979).

[2] Q. Huang, J.F. Zasadzinski, and K.E. Gray, Phys. Rev. B **42,** 7953 (1992).

[3] N. Agraït, J.G. Rodrigo, and S. Vieira, Phys. Rev. B **46,** 5814 (1992).

[4] A.L. de Lozanne, S.A. Elrod, and C.F. Quate, Phys. Rev. B **22,** 2433 (1985); S.A. Elrod, A. Bryant, A.L. de Lozanne, S. Park, D. Smith, and C.F. Quate, IBM Res. Develop. **30,** 387 (1986); J.R. Kirtley, S.I. Raider, R.M. Feenstra, and A.P. Fein, Appl. Phys. Lett. **50,** 1607 (1987); H.F.

Hess, R.B. Robinson, R.C. Dynes, J.M. Valles, Jr., and J.V. Waszczak, Phys. Rev. Lett. **62,** 214 (1989).
[5] Ch. Renner, A.D. Kent, Ph. Niedermann, and O. Fischer, Phys. Rev. Lett. **67,** 1650 (1991).
[6] G.E. Blonder, M. Tinkham, and T.M. Klapwijk, Phys. Rev. B **25,** 4515 (1982).
[7] G.E. Blonder and M. Tinkham, Phys. Rev. B **27,** 112 (1983).
[8] M. Octavio, M. Tinkham, G.E. Blonder, and T.M. Klapwijk, Phys. Rev. B **27,** 6739 (1983); K. Flensberg, J. Bindslev Hansen, and M. Octavio, *ibid.* **38,** 8707 (1988).
[9] K. Flensberg and J. Bindslev Hansen, Phys. Rev. B **40,** 8693 (1989).
[10] J.R. Kirtley, Int. J. Mod. Phys. B4, 201 (1990).
[11] S. Vieira, J.G. Rodrigo, M.A. Ramos, K.V. Rao, and Y. Makino, Phys. Rev. B **40,** 11403 (1989); S. Vieira, J.G. Rodrigo, M.A. Ramos, N. Agraït, K.V. Rao, Y. Makino, and J.L. Costa, J. Appl. Phys. **67,** 5026 (1989).
[12] N. Agrait, J.G. Rodrigo, C. Sirvent, and S. Vieira, Phys. Rev. B **48,** 8499 (1993).
[13] N. Agraït, J.G. Rodrigo, and S. Vieira, Phys. Rev. B **47,** 12345 (1993).
[14] J.K. Gimzewski and R. Möller, Phys. Rev. B **36**, 1284 (1987).
[15] J. Ferrante and J.R. Smith, Surf. Sci. **38,** 77 (1973); M.D. Pashley, J.B. Pethica, and D. Tabor, Wear **100,** 7 (1984).
[16] J.G. Simmons, J. Appl. Phys. **34,** 1793 (1963); N.D. Lang, Phys. Rev. B **37,** 10395 (1988).
[17] U. Dürig, J.K. Gimzewski, and D.W. Pohl, Phys. Rev. Lett. **57,** 2403 (1986); U. Dürig, O. Züger, and D.W. Pohl, *ibid.* **65,** 349 (1990).
[18] R.C. Dynes, V. Narayanamurti, and J.P. Garno, Phys. Rev. Lett. **41**, 1509 (1978); M.A. Ramos and S. Vieira, Physica C **162–164**, 1045 (1989).
[19] J.G. Rodrigo, N. Agraït, and S. Vieira (unpublished).
[20] From the lattice parameters of Pb, we may establish the somewhat conventional correspondence 1 atom $\equiv$ 12.25 Å^2, and from Sharvin resistance formula we obtain the correspondence between atoms and resistances.
[21] Performing the same analysis for the series in Fig. 5 as for the clean series yields the following pairs of [Z,Γ(meV)]: (2.3,0.25), (2.2,0.25), (2,0.25), (1.7,0.2), (1.5,0.2), (1.5,.15), (1.4,0.15), (1.3,0.15), (1.3,0.15), (1.3,0.1).
[22] C.J. Muller, J.M. van Ruitenbeek, and L.J. de Jongh, Physica C **191**, 285 (1992).

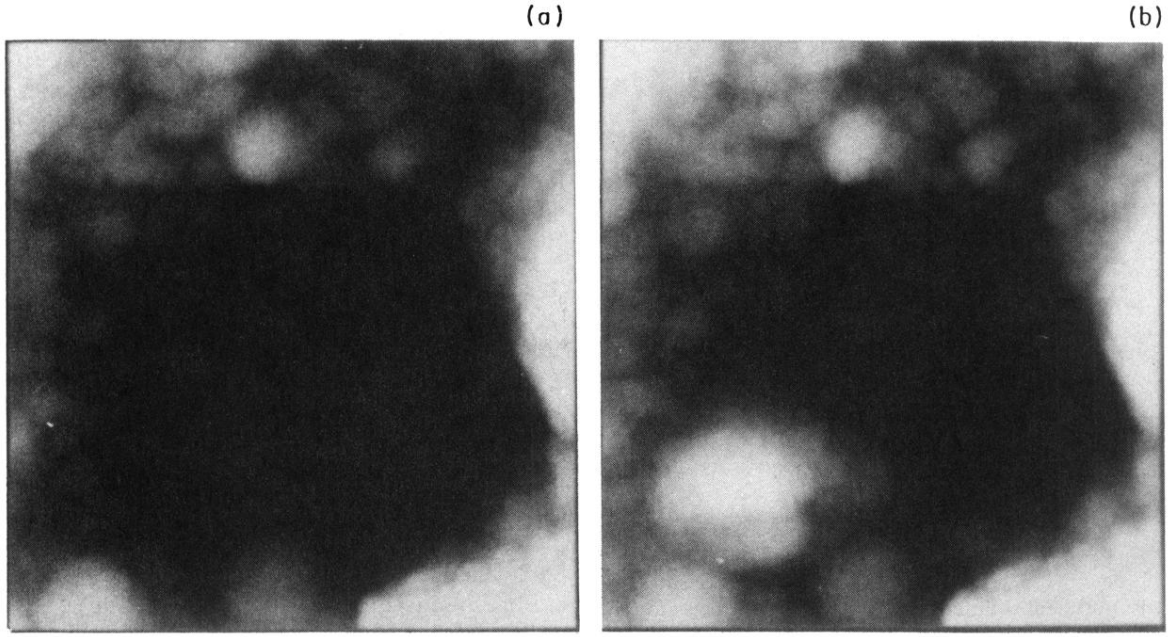

FIG. 1. A typical 50×50 nm^2 area of the Pb substrate at 5.5 K. (a) Before taking any IV curve; (b) after taking several IV curves at 20Ω resistance.